Report: ILIAS–TA project P2007-12-LNGS

Thermal neutron background flux measurements in the underground Gran Sasso National Laboratory.

Zdzisław Dębicki, Karol Jędrzejczak, Jacek Karczmarczyk,
Marcin Kasztelan, Ryszard Lewandowski, Jerzy Orzechowski,
Jacek Szabelski, Maria Szeptycka, Przemysław Tokarski

The Andrzej Sołtan Institute for Nuclear Studies
Poland

Abstract

In April 2008 we measured thermal neutron background flux in the deep underground Gran Sasso National Laboratory. The flux is equal to $(5.31 \pm 1.25) \times 10^{-7}$ neutrons/(cm^2 s). We have used a set of proportional counters filled with ^{3}He. During one week exposure we registered about 650 neutron signals above about 160 background signals, so using this method it would be possible to measure 10 times smaller neutron flux.

This work was supported:
by ILIAS (EU contract RII3-CT-2004-506222) as ILIAS–TA project P2007-12-LNGS,
and by IPJ, Poland

contact person: Jacek Szabelski, js@zpk.u.lodz.pl, tel./fax +(48) 42 6786431
postal address: IPJ, 90–950 Łódź 1, P.O.Box 447, Poland

July 1, 2008

1 Measurements at LNGS.

1.1 Introduction.

At the Gran Sasso National Laboratory (LNGS – Laboratori Nazionali del Gran Sasso) we have performed measurements of thermal neutron flux *"in order to demonstrate the potential sensitivity of the neutron measurement and the alpha background"* (ILIAS Panel recommendation from the letter of November 13, 2007). We made two major runs in the LNGS underground laboratory (further referred as 'tunnel') and 3 calibration runs in the basement of one of the ground level laboratory buildings (see Table 2 on the page 10 in Appendix A). Measurements in the tunnel lasted 17 days and were made in the control room of the former Heidelberg–Moscow double beta decay experiment.

1.2 Detector.

We used 16 proportional gas counters with ^{3}He with nominal pressure 4 atm. We arranged these counters in two ways: one with large exposure and second compact with reduced exposure due to shielding of each detector by the others (see photos – Figure 1). We called the two detectors layouts as 'in line' and 'in circles'. More details about layouts, detector labelling and properties are presented in the Appendix A (page 9).

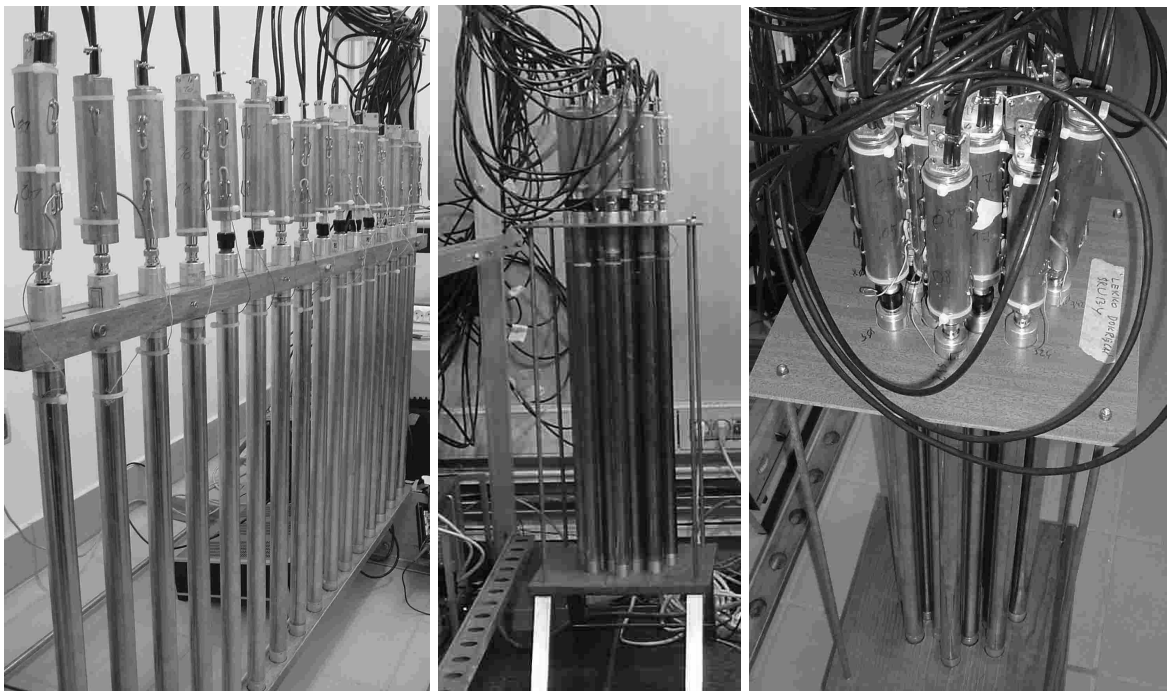

Figure 1: Detector photos. Left photo shows detectors 'in line'. Center and right photos show the compact 'in circles' layout.

The idea of observing low level neutron flux is to see neutron peak at 764 keV above the background level due to α particles emitted inside the detector. In the helium counter the thermal neutrons are registered due to the reaction

$$n +^3 He \longrightarrow p +^3 H + 764keV \tag{1}$$

Amplitudes of signals from ^{3}He counter have characteristic distribution presented in the Figure 2.

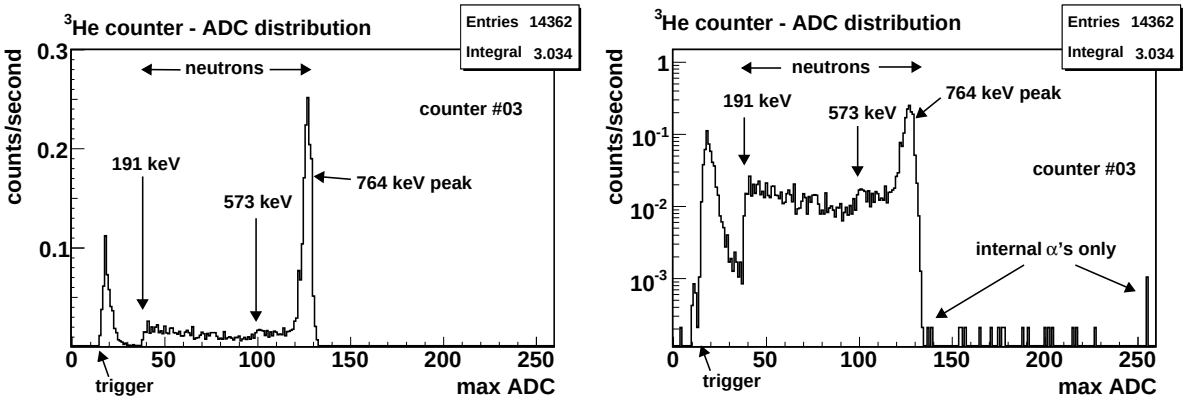

Figure 2: Example of signal maximum amplitude distribution: counting rate in ^{3}He counter. Test measurements made in Poland with AmBe neutron source (emissivity 200 neutrons/s). Counter #03. Left figure in linear scale, and right figure shows the same measurements in log scale. About 60% of neutron related signals are in the 764 keV peak.

More information about neutron registration in ^{3}He proportional counters are in Appendix B (page 12).

In our measurements two ^{3}He counters are connected to one ADC channel. Sixteen ^{3}He counters are connected in pairs to 8 FADC channels (always the same combination of counters, preamplifiers and 10 MHz, 8 bit FADC channels). We adjusted signal amplification in preamplifiers to place the 764 keV neutron peak at maximum ADC level 120 for each counter/preamplifier pair. For measurements in LNGS we set the trigger level (voltage comparator) about the ADC channel 80. Rejecting events with amplitudes below the 764 keV peak we reduced dead time of measurements. For every trigger we store 32 kB wave forms (ADC every 100 ns) from 8 channels, and this lasts 0.7 s. More information about signals and ADCs are presented in the Appendix C (page 13).

2 Thermal neutron flux measurements at LNGS.

2.1 Method of thermal neutron flux measurement.

In order to estimate neutron flux (in neutrons per cm^2·s) it was necessary to compare registered number of neutrons with number of neutrons predicted by computer simulations for assumed neutron flux.
To obtain neutron flux from our registrations we use the relation:

$$N_{obs\ \delta\ i} = f_{\delta\ i} \cdot F_A \cdot 16\pi R^2 \cdot t_{obs\ \delta} \cdot \frac{1}{N_{sim\ \delta}} \cdot \sum_{i-pair} (n_{sim\ \delta\ j} \cdot \kappa_j) \qquad (2)$$

where:
- weighted sum of $f_{\delta\ i} \cdot F_A$ is the neutron flux to be determined,
- F_A is the reference neutron flux used in simulations,
- $f_{\delta\ i}$ is a factor to be evaluated from equation 2,
- δ label indicates detector layout ('in line' or circles),
- i label indicates pair of ^{3}He counters connected to the same ADC channel,
- $N_{obs\ \delta\ i}$ is the number of registered neutrons in the 764 keV peak,

– $t_{obs\ \delta}$ is lifetime (effective registration time),
– R is radius of spherical area of isotropic neutron emission in simulations,
– $N_{sim\ \delta}$ is the number of neutrons emitted in simulations,
– $n_{sim\ \delta\ j}$ is the simulated number of neutrons registered in the j-th counter,
– κ_j is the ratio of number of neutrons in 764 keV peak to the number of all registered neutrons (as presented in the Figure 2, and measured afterwards with the AmBe neutron source, for details see Appendix A on page 9 and Tables 3–5).

Idea of flux measurements is expain in more datails in Appendix D (page 14).

In formula 2 measured values are:

- $N_{obs\ \delta\ i}$ as a difference of the number of signals in 764 keV peak range and the expected α particle background in that range;
- $t_{obs\ \delta}$ as a difference of observation time and dead time (see Table 2 on page 10);
- κ_j as a fraction of neutrons registered in the 764 keV peak (see Figure 2 for example of typical situation).

Simulated values are $n_{sim\ \delta\ j}$ for assumed values of R and $N_{sim\ \delta}$. We take F_A equal to 10^{-6} neutrons/(cm^2 s).

2.2 Neutron and α particle background measurements.

The goal of our measurements was to estimate the number of registered neutrons in the 764 keV peak. However, in the same amplitude range α particles emitted from internal parts of counter produce constant background, as they generate signals indistinguishable from these of neutron origin (equation 1).

2.2.1 Measurement and analysis of α particle background.

The α particles can be clearly registered in ^{3}He proportional counters when their deposited energy in ionisation inside the detector exceeds 764 keV neutron peak. In the counters we had used the observed α particle energy has flat distribution. We assume that this distribution can be extrapolated to the 764 keV peak range.
Results of measurements of α particle background are presented in Appendix E (page 16) and particulrly in the last column in the bottom of the Table 6 (page 17).

2.2.2 Measurements of neutrons in LNGS.

In measurements in the Gran Sasso underground laboratory we made analysis separately in each registration channel. 764 keV peak ranges might be different in each channel (a sum of signals from pair of ^{3}He counters).
During one week measurements with counters in 'line' layout we found 811 events in 764 keV peak. We estimated that the number of neutrons was 657.7, and the number of expected signals due to α particle background was 154.9. Neutron rate (in 764 keV peak) from 16 counters was 4.2 per hour, and related α particle rate was 0.98 per hour.
During 10 days measurements with counters in 'circles' layout in the inner circle detectors (8 counters) we found 335 events in 764 keV peak, with 228.6 neutrons (rate 1.00 per hour) and 108.0 α particles (rate 0.47 per hour).
In the outer, more exposed circle (8 counters) we found 445 events in 764 keV peak range, with 326.0 neutrons (rate 1.42 per hour), and 121.5 α particles (rate 0.53 per hour).
The sum of estimated number of neutrons and number of α particle background does not need to be equal exactly to the number of events observed due to the method used

in evaluation of number of neutrons. For more details of data analysis see Appendix F (page 17).

2.3 Simulations.

We used GEANT4 toolkit [1] to simulate efficiency of neutron rejestrations in ^{3}He counters. To find expected number of neutrons registered in LNGS measurements (i.e. numbers $n_{sim\ \delta\ j}$ in equation 2) we simulated registration in layout 'in line' and separately 'in circles' emitting 0.024 eV neutrons isotropically from the sphere with radius $R = 3$m. We made simulations for the same ^{3}He gas pressure (4 atm) in each detector, and for variable pressure adjusted to calibration measurements made for each detector in Poland using AmBe neutron source and neutron moderator – assuming that the difference of efficiency between detectors is due to difference in ^{3}He gas pressure.
Datailed results of simulations are presented in the Appendix G (page 22).

In comparison between measurements and expected values from simulations we also included the values of fraction of neutrons in the 764 keV peak (from the whole neutron range: 191–764 keV). This fraction (κ_j in equation 2) was measured in counter calibrations with AmBe source and neutron moderator.

3 Thermal neutron flux estimation.

Neutron flux can be evaluated by comparison of neutron registrations with simulations normalised for expected neutron flux (see equation 2). Results are presented in the Table 1.

Neutron registrations in the tunnel were made effectively in 3 different conditions: line, inner circle and outer circle and were presented in Tables 8, 9 and 10 respectively (page 21 in the Appendix F, where there are more details about data analysis). Effective time of measurements is shown in the Table 2.

Table 1: Results of thermal neutron flux measurements. Overall result was obtained as the mean value of $f_{\delta\ i} \cdot F_A$ (equation 2) from both runs in the tunnel: 8 points (channels) from 'in line' measurements and 8 points from 'in circles' setup.

	average flux $\left(10^{-7} \times \frac{\text{neutrons}}{\text{cm}^2\text{s}}\right)$
overall result	**5.309 ± 1.250**
'in line'	5.671 ± 1.141
inner circle	5.017 ± 1.324
outer circle	5.166 ± 1.250
overall result without statistical weigths	5.395 ± 1.251

The role of simulation with different assumptions about ^{3}He counter properties on estimation of low energy neutron flux is presented in the Appendix H.

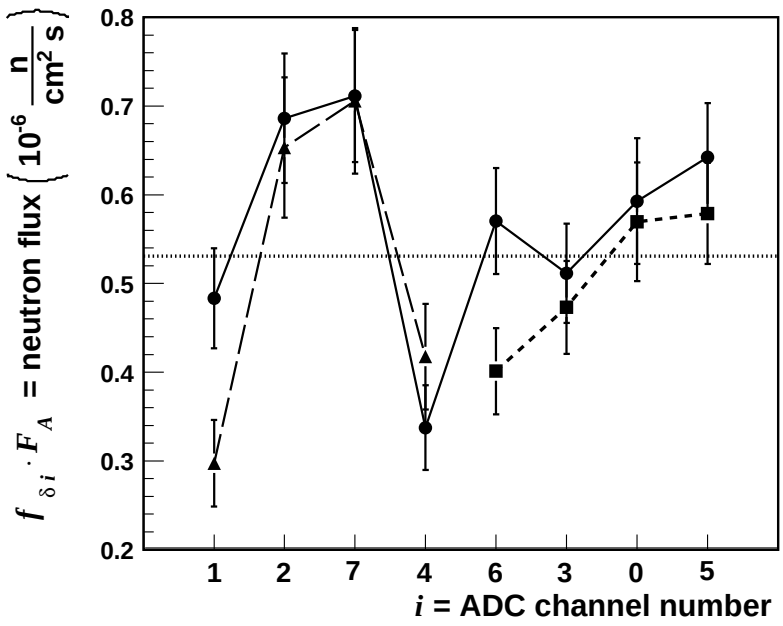

Figure 3: Average neutron flux (horizontal dotted line) and flux values ($f_{\delta\ i} \cdot F_A$ from equation 2) obtained from comparison of simulations and measurements for separate ADC channels. Circles connected by solid line correspond to layout 'in line', triangles connected by large broken line represent inner circle, squares connected by broken line are for outer circle in 'circles' layout. Indicated errors are statistical, only.

In the Figure 3 we present the ratio of measured rate to the expected rate for the neutron flux equal to 10^{-6} n/(cm^{-2} s) (i.e. $f_{\delta\ i} \cdot F_A$ from equation 2), for each ADC channel separately and for the simulation case, when difference in ^{3}He gas pressure was adjusted individually and fraction of neutrons in the 764 keV peak was measured. This rate is estimated thermal neutron flux as it would be when measured in single channel. The distribution of all points (i.e. from layouts 'in line' and 'in circles') is presented in the Figure 4.

4 Discussion.

We evaluated neutron flux by comparison of neutron registrations with simulations normalised to unit neutron flux (see equation 2). During 17 days we exposed our detectors to thermal neutron background in two layouts: for a week with high neutron registration efficiency (setup 'in line') and for 10 days in setup 'in circles' (see Figure 6 on page 10 in the Appendix A) where counters registering neutrons also shielded other counters from neutrons from particular directions. Detector is less efficient in thermal neutron registration than was in 'in line' setup. For half of counters placed inside in 'circle' setup we expected smaller efficiency than for counters which form the outer circle. The effect is present only for thermal neutrons for which counters are almost 'dark' due to large cross section for reaction (1). Results obtained in measured 3 different counting rates support our assumption: we measured thermal neutrons and our expected neutron rates from GEANT4 simulations are 'reasonable'.

We obtained the thermal neutron flux equal to $(5.31 \pm 1.25) \times 10^{-7}$ neutrons/(cm^2 s). We do not know other neutron flux measurements in that energy range in Gran Sasso. In the Figure 5 we present results of neutron flux measurements in MeV range [3] and our

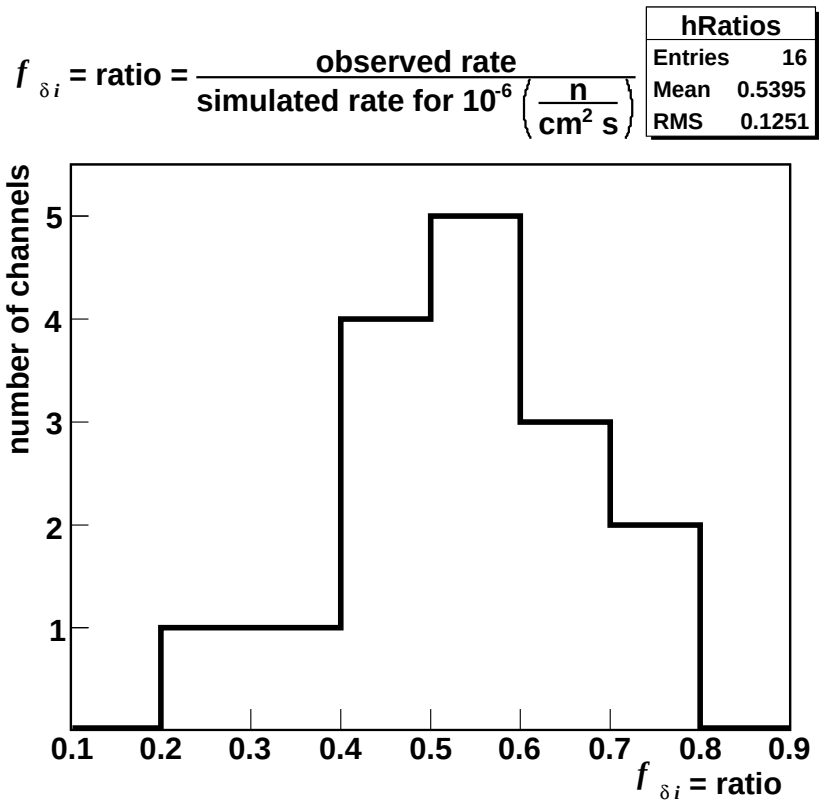

Figure 4: Distribution of ratios of measured neutron rate to expected rate for each channel separately (i.e. $f_{\delta\ i}$ from equation 2) for measurements 'in line' and 'in circles'. In simulations of expected neutron rates the individually adjusted ^{3}He pressure was used. Measured fraction of neutrons in 764 keV peak was applied.
The mean value shown in this figure does not include statistical weights.

result (Figure 5 does not present neutron flux energy spectrum). The MeV energy range measurements were made using different scintillation technics. Probably different parts of the underground laboratory have different neutron background.

4.1 Error analysis.

Error of thermal neutron flux is a result of distribution of flux values ($f_{\delta\ i} \cdot F_A$ from equation 2) obtained for each channel and for two runs (16 values). The distribution is presented in the Figure 4. Situation is presented better in the Figure 3, where values $f_{\delta\ i} \cdot F_A$ for the same combination: channel, counter and amplifier (labelled in the figure according to channel number) were compared for two runs: 'in line' and 'in circles'. Errors indicated in the Figure 3 refer to statistical errors due to number of neutrons registered in the 764 keV peak above α particle background. 5/8 measurements in the same channel are within statistical errors, which look statistically correct.

Results from channels 1, 2, 7 and 4 have very wide distribution of $f_{\delta\ i} \cdot F_A$. Results from channels 6, 3, 0 and 5 are more consistent.
We do not know what was the reason for so wide distribution of $f_{\delta\ i} \cdot F_A$ from channels 1, 2, 7 and 4. The value $f_{\delta\ i} \cdot F_A$ depends on measurement results and on simulation results. Comparing measured neutron rates from channels 1 and 2 for measurements with layout 'in line' made in the laboratory building outside the tunnel (Table 7 on page 21 in the

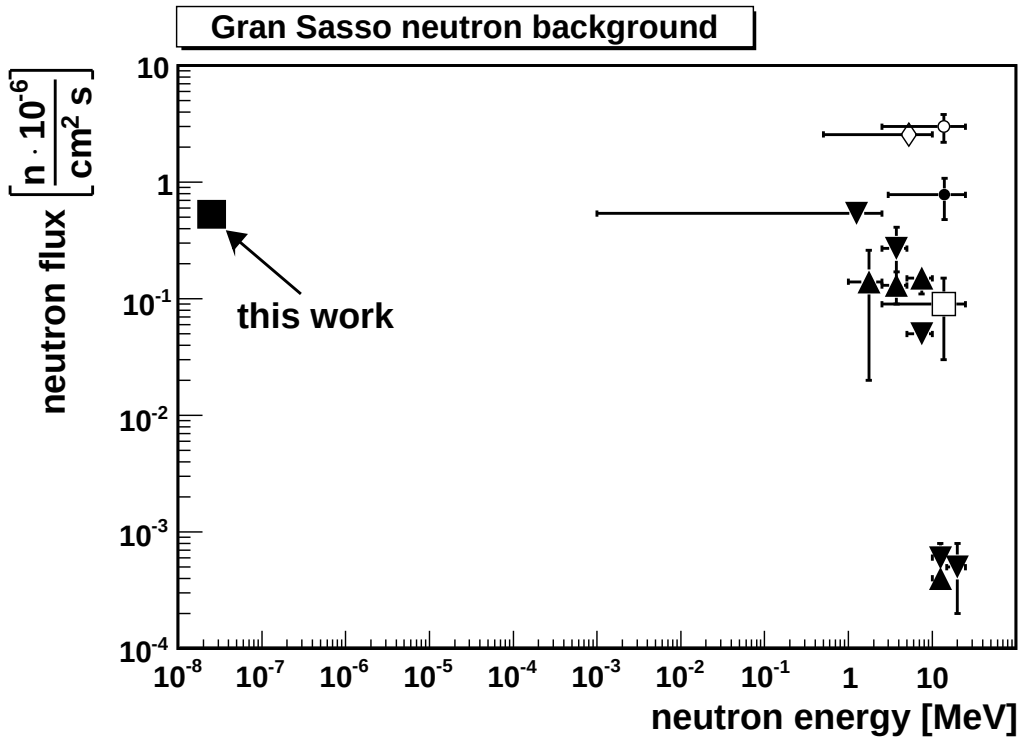

Figure 5: Compilation of neutron background measurements in the underground Gran Sasso Laboratory. MeV range neutron flux measurements were drawn according to work of H. Wulandari et al. [3].

Appendix F) with results from measurements in the tunnel (Table 8, page 21) we can see that neutron rate in channel 1 exceeds neutron rate in channel 2 for surface measurement contrary to results from the tunnel. For measurements with 'in line' setup made in surface laboratory after measurements in the tunnel neutron rates from channels 1 or 4 are higher than from channels 2 or 7.

We also consider the possibility that thermal neutron flux in the tunnel might not be isotropic. If we compare a map of counters shown in Figure 6 (page 10) with Figure 3 we would find that counters at the bottom of the map in Figure 6 (channels 2,7 for inner circle and channels 0, 5 for outer circle) had shown an excess of $f_{\delta\ i} \cdot F_A$ values over counters at the top of the map. However, the effect is not consistent with measurements in 'line' setup.

We examined the stability of neutron and alpha registrations. We found that counting rates in time were stable in each channel. We found that the distribution of time difference between subsequent registration of neutron or alpha have exponential form, as expected.

We conclude that the flux error we quote reflects unknown systematic difference between detectors efficiency. These differences were not stable, and were not seen in runs in surface laboratory.

4.2 Background due to α particles in a 764 keV peak range and limits for neutron flux measurements.

The α particle background was described in the Appendix E (page 16). We can measure this background only in the maximum ADC range above 764 keV peak. Then we extrapo-

lated the background level (in each channel separately) to the maximum amplitude range of 764 keV neutron peak. The results of these procedures were summarized in Tables 7, 8, 9 and 10 on pages 21–22 in the Appendix F.

Shielding detectors in layout similar to that 'in circles' by the thermal neutron absorber it would be possible to reduce neutron flux and to measure in deep underground laboratory α particle background in the maximum ADC range of neutron registration.
We have not observed any lines in ADC distribution for counters we had used in LNGS, but we had observed such lines (above 764 keV peak) in other counters.

If there would be no extra lines from internal α particle background in maximum ADC distribution we can estimate the lower measurable thermal neutron flux which can be measured in 'line' setup. In one week exposure in the tunnel (Table 8) the sum of α particle background in 764 keV peak range was about 160 events. Therefore thermal neutron flux on the level $5.3{\cdot}10^{-8}$ neutrons/(cm^2 s) (i.e. 10 times smaller than measured in this work) would give about 66 neutron counts in 764 keV peak area, which would be about 5σ excess above the α background.
As we learned a lot during these measurements in LNGS we would make next registration system better, i.e. separate ADC per counter would ensure narrower 764 keV peak distribution.

4.3 Conclusions.

We hope that our results would be useful in neutron background analysis and simulations made for the Gran Sasso laboratory.

5 Acknowledgement

Authors would like tank Mr. Wojciech Starosta from the Institute of Nuclear Chemistry and Technology (IChTJ) for lending us his ^{3}He counters.
We are grateful to Dr. Stanisław Pszona from IPJ for low emissivity AmBe neutron source and many discussions about ^{3}He counters and neutron detections.
We thank Prof. Joanna Stepaniak from IPJ for contacting us with ILIAS.
We thank Mr. Adam Kaźmierski Dr. Adam Konefał, and Dr. Tadeusz Kozłowski for helpful discussions.
This work was supported by ILIAS (EU contract RII3-CT-2004-506222) as ILIAS–TA project P2007-12-LNGS and by IPJ, Poland.

References

[1] S. Agostinelli et al., Nuclear Instruments and Methods in Physics Research **A506**, #3 (2003), 250–303

[2] J. W. Marsh, D. J. Thomas and M. Burke Nuclear Instruments and Methods in Physics Research **A366**, #2 (1995), 340–348

[3] H. Wulandari et al., hep-ex/0312050 v.2, 19 June 2004

A List of runs at LNGS and detector overview.

The Table 2 (page 10) summarizes dates and time of our neutron measurements at LNGS.

Table 2: List of runs of neutron background measurements at LNGS. Runs are in time sequence.

	LNGS lab line #1	LNGS tunnel line	LNGS tunnel circles	LNGS lab circles	LNGS lab line #2	sum all runs	sum tunnel
start–date	2008-04-05	2008-04-07	2008-04-14	2008-04-24	2008-04-25		
start–time	21:34:36	18:39:14	18:13:46	20:59:43	13:20:42		
stop–date	2008-04-06	2008-04-14	2008-04-24	2008-04-25	2008-04-25		
stop–time	09:46:32	10:20:53	11:15:29	11:13:08	19:10:07		
number of triggers	27000	11040	17790	24240	12080		
time (s)	43912	574881	838845	51201	20964	1529803	1413726
time (h)	12.20	159.69	233.01	14.22	5.82	424.95	392.70
lifetime (s)	25012	567153	826392	34233	12508	1465298	1393545
lifetime (h)	6.95	157.54	229.55	9.51	3.47	407.03	387.10

Sixteen ^{3}He proportional counters were connected to eight inputs of ADC channels. The combinations of detector, preamplifier, and ADC channel were the same in all measurements.

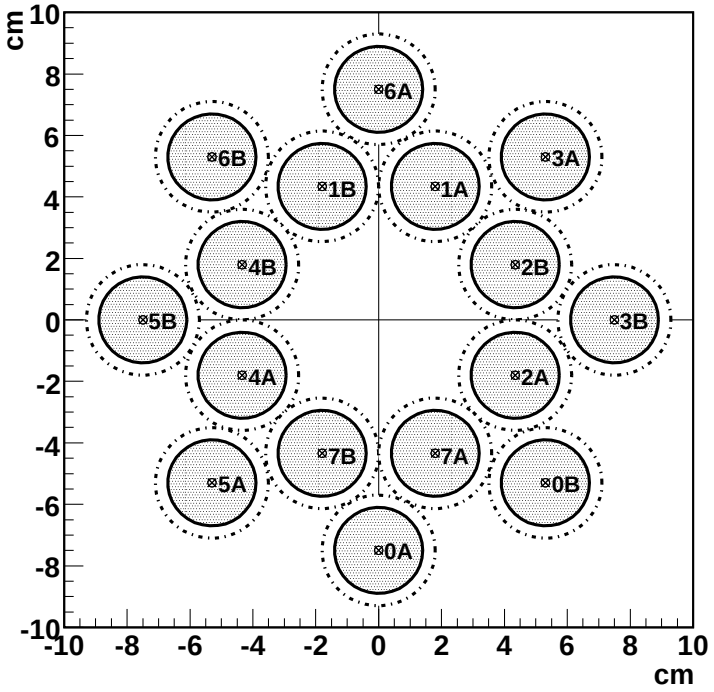

Figure 6: Map of detector layout 'in circles'. Inner shadowed circles are ^{3}He detectors, outer dashed–dotted circles indicate preamplifier sizes. Labels indicate connections to channels.

In Tables 3, 4, and 5 layouts and some parameters of detectors were presented. Detector parameters: fraction of neutrons in 764 keV peak, relative width of the 764 keV peak, and observed rate of neutrons from the test with the AmBe neutron source were obtained from the laboratory measurements after return from LNGS. The observed rate of neutrons is the difference between the rate measured with AmBe source and without the source. Detectors were placed one by one in the same position in the calibration setup: graphite

Table 3: Detector labelling and properties, in order of channel number.
In 'circle' layout column label 'M' indicates inner smaller circle, and 'D' outer larger circle. Neutron fraction in 764 keV peak – κ_j refers to equation (2) and (6).

FADC channel label	^{3}He counter label	pre–amplifier label	# 'line'	# 'circles'	κ_j neutron fraction in 764 keV peak	764 keV peak width	rate with AmBe
0A	08	06	11	5D	0.589	0.041	2.14
0B	05	05	10	4D	0.576	0.045	2.26
1A	327	02	1	1M	0.636	0.060	2.53
1B	330	01	0	0M	0.614	0.057	2.42
2A	06	18	5	3M	0.569	0.036	2.39
2B	03	17	4	2M	0.581	0.036	2.26
3A	324	07	6	2D	0.634	0.058	2.39
3B	332	08	7	3D	0.716	0.066	2.48
4A	336	11	12	6M	0.665	0.055	2.41
4B	338	12	13	7M	0.658	0.064	2.14
5A	333	13	14	6D	0.682	0.039	2.46
5B	334	14	15	7D	0.669	0.038	2.65
6A	342	09	2	1D	0.632	0.048	2.39
6B	340	10	3	0D	0.743	0.096	2.46
7A	07	15	8	4M	0.581	0.043	2.18
7B	04	16	9	5M	0.596	0.063	2.29

Table 4: Detector labelling and properties, in order of position in 'line' layout. In 'circle' layout column label 'M' indicates inner smaller circle, and 'D' outer larger circle. Neutron fraction in 764 keV peak – κ_j refers to equation (2) and (6).

FADC channel label	^{3}He counter label	pre–amplifier label	# 'line'	# 'circles'	κ_j neutron fraction in 764 keV peak	764 keV peak width	rate with AmBe
1B	330	01	0	0M	0.614	0.057	2.42
1A	327	02	1	1M	0.636	0.060	2.53
6A	342	09	2	1D	0.632	0.048	2.39
6B	340	10	3	0D	0.743	0.096	2.46
2B	03	17	4	2M	0.581	0.036	2.26
2A	06	18	5	3M	0.569	0.036	2.39
3A	324	07	6	2D	0.634	0.058	2.39
3B	332	08	7	3D	0.716	0.066	2.48
7A	07	15	8	4M	0.581	0.043	2.18
7B	04	16	9	5M	0.596	0.063	2.29
0B	05	05	10	4D	0.576	0.045	2.26
0A	08	06	11	5D	0.589	0.041	2.14
4A	336	11	12	6M	0.665	0.055	2.41
4B	338	12	13	7M	0.658	0.064	2.14
5A	333	13	14	6D	0.682	0.039	2.46
5B	334	14	15	7D	0.669	0.038	2.65

walls and water moderator inside. ^{3}He counter and AmBe source were placed inside graphite walls, near to moderator. The DAQ was different (faster) than used in LNGS measurements, however with very similar registration principle: 16 MHz, 8 bit resolution ADC.

Table 5: Detector labelling and properties, in order of position in 'circle' layout. In 'circle' layout column label 'M' indicates inner smaller circle, and 'D' outer larger circle. Neutron fraction in 764 keV peak – κ_j refers to equation (2) and (6).

FADC channel label	^{3}He counter label	pre–amplifier label	# 'line'	# 'circles'	κ_j neutron fraction in 764 keV peak	764 keV peak width	rate with AmBe
1B	330	01	0	0M	0.614	0.057	2.42
1A	327	02	1	1M	0.636	0.060	2.53
2B	03	17	4	2M	0.581	0.036	2.26
2A	06	18	5	3M	0.569	0.036	2.39
7A	07	15	8	4M	0.581	0.043	2.18
7B	04	16	9	5M	0.596	0.063	2.29
4A	336	11	12	6M	0.665	0.055	2.41
4B	338	12	13	7M	0.658	0.064	2.14
6B	340	10	3	0D	0.743	0.096	2.46
6A	342	09	2	1D	0.632	0.048	2.39
3A	324	07	6	2D	0.634	0.058	2.39
3B	332	08	7	3D	0.716	0.066	2.48
0B	05	05	10	4D	0.576	0.045	2.26
0A	08	06	11	5D	0.589	0.041	2.14
5A	333	13	14	6D	0.682	0.039	2.46
5B	334	14	15	7D	0.669	0.038	2.65

B Neutron registration principle.

The idea of observing low level neutron flux is to see neutron peak at 764 keV above the background level due to α particles emitted inside the detector. In the helium counter the thermal neutrons are registered due to the reaction

$$n +^3 He \longrightarrow p +^3 H + 764keV \tag{3}$$

The cross section for this reaction can be parameterized in low energy region:

$$log_{10}(\sigma/barn) = 2.92 - log_{10}(En/eV)/2 \tag{4}$$

The thermal neutron energy (∼0.024 eV) is negligible compared with reaction energy. The reaction energy is taken by proton (573 keV) and tritium (191 keV). In our counters (made in our Institute – ZDAJ IBJ in the 70–ties) the 0.5 atm of krypton (Kr) was added to enforce ionisation losses. When one of reaction products reaches the counter walls some reaction energy is missed in registration, and the characteristic effect is called "wall effect". Energies due to thermal neutron registration in helium counter are in range from 191 keV to 764 keV with characteristic peak near to 764 keV. For our counters for about 60% of events the whole reaction energy is observed. See Figure 2 for example of counter performance and Tables 3, 4 or 5 for all counters summary data.

The α particles emitted inside the detector produce signals similar to those from neutron registrations. The distribution of energies is approximately flat up to about 5–6 MeV. It is possible to measure these particles when α energy is greater than neutron peak energy (764 keV). Results of measurements of α distribution in counters (channels) as they were used in LNGS are described in Section E (page 16). In the neutron energy range neutron signal dominates, unless the measurements are made in very low neutron background environment. Therefore in low neutron intensity measurements it is important to use detectors with narrow 764 keV neutron peak and with most of neutrons registered with

full reaction energy.

Our measurement set-up places amplitudes of 764 keV neutron peak near to the level 120 of ADC. The ADC range is from 0 to 255, and the no–signal noise level (offset) is at level 8–10. Therefore particle energies above about 1700 keV give saturation of ADC.

In our measurements two ^{3}He counters are connected to one ADC channel. Sixteen ^{3}He counters are connected in pairs to 8 FADC channels (always the same combination of counters, preamplifiers and 10 MHz, 8 bit FADC channels).

C Signal processing.

^{3}He counters were connected to HV = 1200 V through preamplifier. Preamplifiers were connected (BNC connection) directly to the counters. Signals were amplified about 400 times there. Amplification was adjusted in each preamplifier/counter set during calibration runs to obtain similar signals for 764 keV peak from each counter (i.e. each counter separately, not pair of counters).

The differential symmetric signals from preamplifiers were transmitted through pair of twisted cables (about 3 m long) to CAMAC ADC block. Two preamplifiers/counters were connected to one FADC input. 50 Ω terminators were on outputs from preamplifiers, only.

The CAMAC block has 8 FADC channels. Each input can trigger registrations from all channels. The sampling rate is 10 MHz, ADC is 8 bit (0–255) range for about 0–1 V signal range, and each channel has 32kB buffer for each registration. The trigger was placed in 1536$^{\text{th}}$ 100 nsec pixel, which allows to view about 150 μsec before trigger. Figure 7 shows example of neutron signal registration, and computer analysis of the signal. Examining of signal front was essential in removing rare events from micro sparcs from high voltage occuring near to BNC connection between preamplifier and the counter.

Transmission of single event (i.e. 8 × 32kB) from CAMAC to 'on line' PC computer lasts 0.7 sec. This is dead time present after each event. In principle we could reduce the buffer size to 8kB without reducing detection performance for neutron background measurements. However, we like to search for multiple neutron events within a few miliseconds – we have observed such events in our laboratory. During measurements in LNGS we have not found multiple neutron events.

The maximum ADC for the signal was evaluated as maximal value of running average from subsequent 7 ADC pixels. From the bottom Figure 7 it can be seen, that the ADCs are near to maximum for sufficiently long time, and the maximum ADC can be measured precisely.
The amplification of the preamplifiers was adjusted to place the 764 keV peak amplitude at the ADC level equal to 120.

The trigger is made as input signal voltage comparator. The comparators, one per channel, are placed in FADC block. For measurements in LNGS we adjust the trigger signal level around channel 80. Therefore we lost most of the neutron signals corresponding to 'wall effect' amplitudes. This way we try to reduce dead time. However, now, after the measurements, we think that we could set the trigger level much lower.

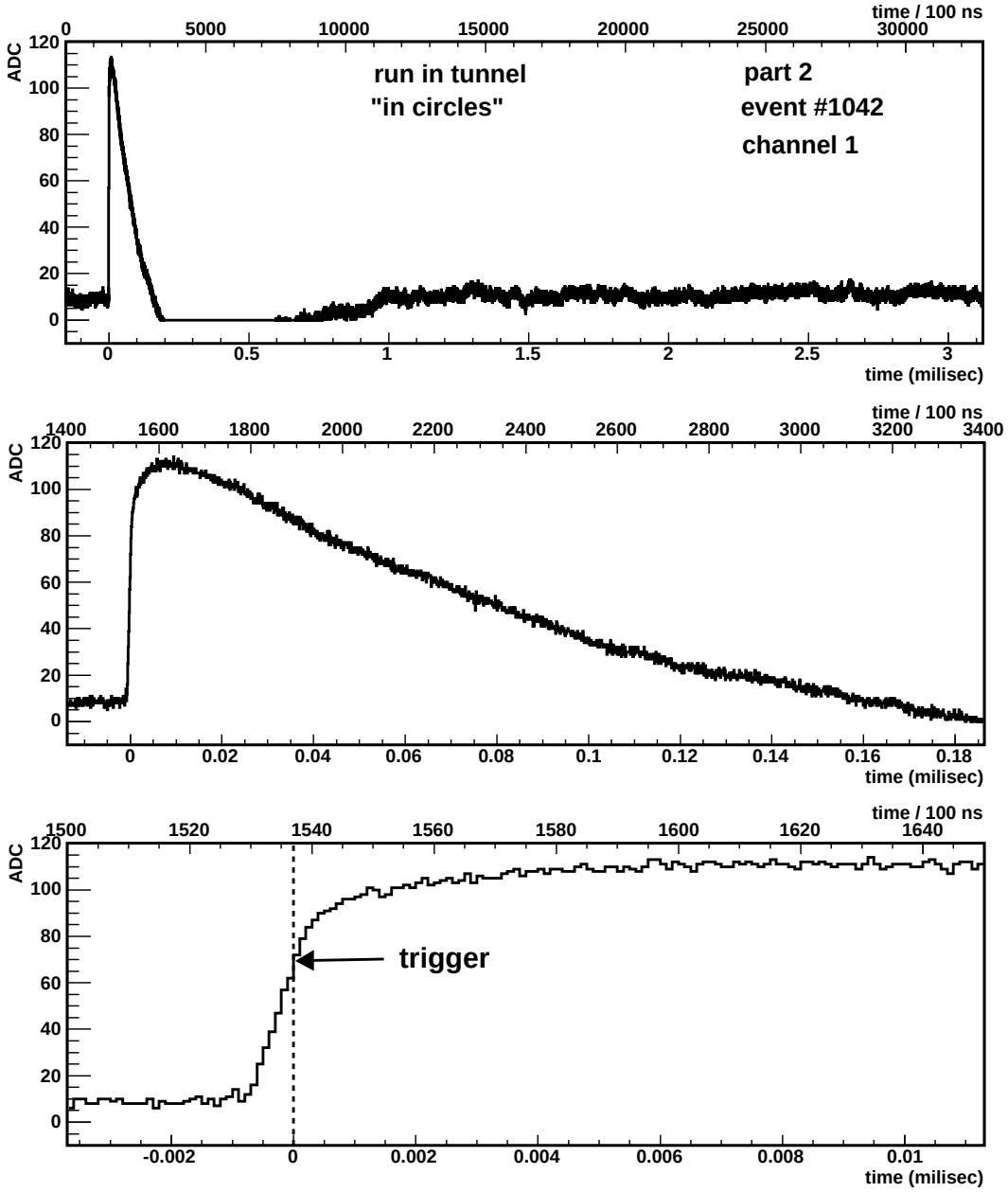

Figure 7: Example of registered signal. Top figure shows whole wave form. Center figure shows part of the top figure: the neutron like signal. Bottom figure shows the front of the neutron signal (or α signal), and the position of the trigger is indicated.

D Method of thermal neutron flux evaluation: result of measurements and simulations.

In order to estimate neutron flux (in neutrons per $cm^2 \cdot s$) it was necessary to compare registered number of neutrons with number of neutrons predicted by computer simulations for assumed neutron flux. Simulations were performed using GEANT4 toolkit [1].

In measurements two ^{3}He counters were connected to the same FADC input channel. Observed neutron number in each channel was the sum of neutrons registered in 2 counters. Always the same pair of counters were connected to the same FADC input channel.

There were two experiment runs in the LNGS underground laboratory. For the first run detectors were placed 'in line', and therefore each detector had large exposure. For the second run detectors were placed closely in 'two circles', so the ^{3}He gas acted also as neutron absorber. All detectors where partially shielded, and detectors from the inner circle more than those from outer circle. Both detector layouts were simulated. We expect 3 different neutron registration efficiencies. Therefore we had 3 neutron flux measurements.

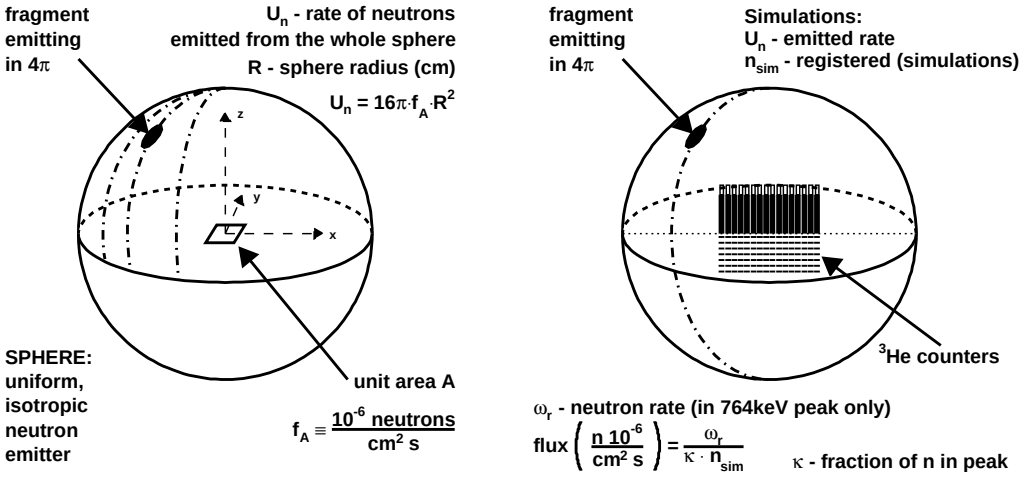

Figure 8: Idea of simulations.
Left figure shows the idea of normalisation to reference neutron flux F_A. Only emission from half of sphere is included. Right figure refers to simulations with detectors.

In simulations (GEANT4) thermal neutrons (neutrons with energy 0.024 eV) were emitted isotropically (4π) from each point uniformly chosen from the points on the sphere of radius $R = 3$ m (see Fig. 8). The detectors were placed centrally inside the sphere. Neutron intensity was uniform over the volume occupied by detectors with accuracy better than 2%. Simulations with detectors were performed for two detector layouts: 'in line' and 'circles'. The required emitted neutron rate (from the whole sphere) U_n corresponds to the reference neutron flux F_A, and is equal to:

$$U_n = 16\pi R^2 \cdot F_A \tag{5}$$

since

$$F_A \cdot A = \int_0^{2\pi} \int_0^1 \frac{A cos(\theta)}{4\pi R^2} \cdot \frac{U_n}{4\pi}\ dcos(\theta)\ d\phi = \frac{U_n A}{16\pi R^2}$$

where

- A is small surface area,
- $U_n/4\pi$ is a emissivity density per steradian,
- $U_n/4\pi \cdot dcos(\theta)\ d\phi$ is emissivity from infinitesimal surface area, and
- $Acos(\theta)/4\pi R^2$ is a fraction of the sphere occupied by the surface A, as seen from isotropically emitting point with (θ, ϕ).

Integration is over the nothern hemisphere, only, since the flux is 'one way' by definition. We use $F_A = 10^{-6} \frac{\mathrm{n}}{\mathrm{cm^2 s}}$ and $R = 3$ m in our simulations.

To obtain neutron flux from our registrations we use the relation:

$$f_{\delta\ i} \cdot F_A = \frac{N_{obs\ \delta\ i}}{16\pi R^2 \cdot t_{obs\ \delta} \cdot \frac{1}{N_{sim\ \delta}} \cdot \sum_{i-pair} (n_{sim\ \delta\ j} \cdot \kappa_j)} \tag{6}$$

where:

- weighted sum of $f_{\delta\ i} \cdot F_A$ is the neutron flux to be determined,
- F_A is the reference neutron flux used in simulations,
- $f_{\delta\ i}$ is a factor to be evaluated from equation 2,
- δ label indicates detector layout ('in line' or circles),
- i label indicates pair of ^{3}He counters connected to the same ADC channel,
- $N_{obs\ \delta\ i}$ is the number of registered neutrons in the 764 keV peak,
- $t_{obs\ \delta}$ is lifetime (effective registration time),
- R is radius of spherical area of isotropic neutron emission in simulations,
- $N_{sim\ \delta}$ is the number of neutrons emitted in simulations,
- $n_{sim\ \delta\ j}$ is the simulated number of neutrons registered in the j-th counter,
- κ_j is the ratio of number of neutrons in 764 keV peak to the number of all registered neutrons (as presented in the Figure 2, and measured afterwards with the AmBe neutron source, for details see Appendix A on page 9 and Tables 3–5).

Elements of equation 6 are discussed separately in this report.

E Background due to α particles.

Registration of α particles emitted from inside the detector is a constant background. Energies of these particles are from 0 to about 5–6 MeV. These α particles might come from metallic body of the ^{3}He detector, wolfram wire, ceramic sealing or gas, if these components contain some additions of radioactive elements. Radioactive additions in gas would produce lines in maximum ADC distribution, and we have not observe such effect in these couters for ADC higher than 764 keV peak.

E.1 Background in energy range 830–1650 keV.

Here we summarize α particle rates in different runs and separately in each channel. In this section we examine amplitudes in the range 130–250 (approximate energy range 830–1650 keV), i.e. above 760 keV neutron peak, and below saturation of ADC.
In the Table 6 we put down results of measurements of α particle background with following selection criteria:

1. signal starts rising at trigger position (1536);
2. signal reaches its maximum later than in pixel 1580, i.e. later than 44 pixels (= 4.4 μsec) after trigger;
3. the ADC maximum amplitude is in the range 130–250 (both included).

As the transmission of every event lasts 0.7 sec, this is a dead time related to every trigger registration. Therefore the life time of measurements is the difference of clock time and the sum of dead time (0.7 sec $\times$ no of triggers). Table 2 contains time information, and the run lifetimes are included in the lower part of Table 6.

Table 6: α particles in ^{3}He detectors. Values of α particles relate to ADC amplitude range 130–250 only. See subsection E.1 for more information.
G – indicates pairs of ^{3}He counters with bigger connectors.
(*) – applied time corrections due to fault in one of runs.

	FADC channel	LNGS lab line #1	LNGS tunnel line	LNGS tunnel circles	LNGS lab circles	LNGS lab line #2	sum	sum tunnel
number of events	#0 G	3	184	274	6	14	481	458
	#1	15	252	383	0	7	657	635
	#2 G	5	117	149	8	4	283	266
	#3	15	191	278	14	6	504	469
	#4	9	206	299	23	4	541	505
	#5	19	176	257	16	6	474	433
	#6	16	177	239	22	18	472	416
	#7 G	10	147	248	17	4	426	395
rates per hour run time	#0 G	0.246	1.152	1.176	0.422	2.405	1.132	1.166
	#1	1.230	1.578	1.644	—	1.203	(*)1.600	1.617
	#2 G	0.410	0.733	0.639	0.563	0.687	0.666	0.677
	#3	1.230	1.196	1.193	0.985	1.031	1.186	1.194
	#4	0.738	1.290	1.283	1.617	0.687	1.273	1.286
	#5	1.557	1.102	1.103	1.125	1.031	1.115	1.103
	#6	1.311	1.108	1.026	1.547	3.093	1.111	1.059
	#7 G	0.820	0.921	1.064	1.195	0.687	1.002	1.006
rates per hour lifetime	#0 G	0.432	1.168	1.194	0.631	4.035	1.182	1.183
	#1	2.158	1.600	1.668	—	2.017	(*)1.653	1.640
	#2 G	0.719	0.743	0.649	0.841	1.153	0.695	0.687
	#3	2.158	1.212	1.211	0.472	1.729	1.238	1.212
	#4	1.295	1.308	1.303	2.419	1.153	1.329	1.305
	#5	2.734	1.117	1.120	1.682	1.729	1.165	1.119
	#6	2.302	1.124	1.041	2.313	5.187	1.160	1.075
	#7 G	1.439	0.933	1.080	1.788	1.153	1.047	1.020

F Registration of neutrons at LNGS.

Measurements in the tunnel were made in the control room of the former Heidelberg–Moscow double beta decay experiment. We performed two runs with linear layout of detectors and with 'circles' layout. See Table 2 for time of measurements, and Figures 1 and 6 for layout images.

Before detector was placed in the underground laboratory, we made a few short calibration runs in the basement of one of the surface LNGS laboratory building. The task was to adjust amplification of signal and set 764 keV neutron peak at the 'max ADC' level of 120. These was done separately for each counter.
The amplitude trigger level was set to about level 80 of ADC so we cut large part of neutron signals from the area of the 'wall effect' (see Figures 2). The reason was to reduce the dead time (0.7 sec for each trigger) since we plan to use in analysis only signals from 764 keV peak.

Then we made an overnight calibration run in the surface laboratory (see Table 2), and results are presented in the Figure 11.
Next day we moved and reinstalled detectors in the underground laboratory (for the sequence of LNGS runs see Table 2).

Figures 9 and 10 show measured max ADC distribution in the region near to 764 keV

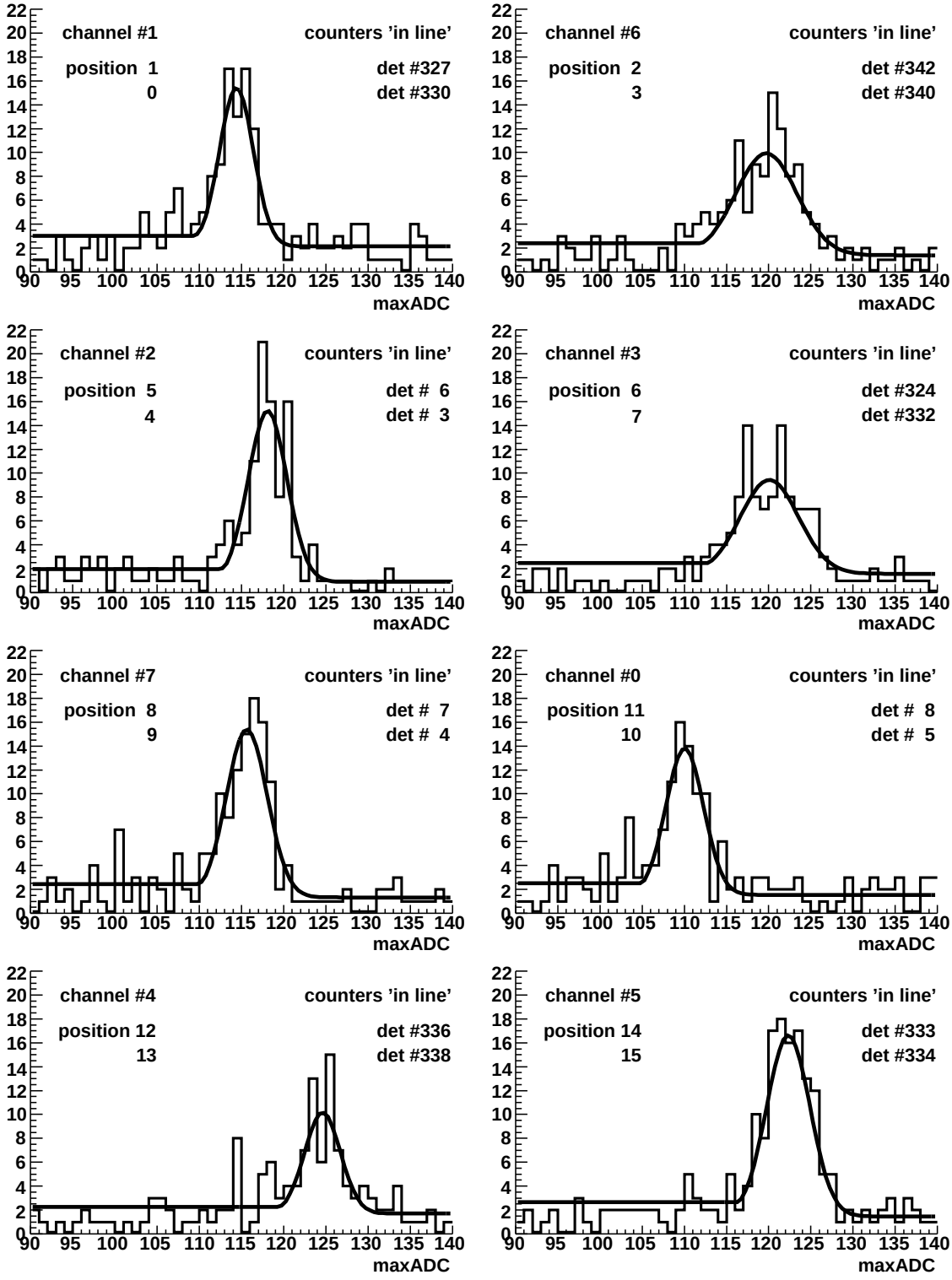

Figure 9: Neutron registrations in underground laboratory and detector setup 'in line'. There are separate distributions for each ADC channel. Order of figures corresponds to detector setup 'in circles', in the Figure 10 and position of detectors in 'line' setup are indicated by numbers from 0 to 15. Pairs of detectors are connected to one channel.
Fit is sum of gaussian distribution for 764 keV peak, α background constant level (see Table 6), and 'wall effect'.

peak for each channel separately (but for two ^{3}He counters, as indicated).
Fits to the distributions were shown. The fit is sum of 3 components:

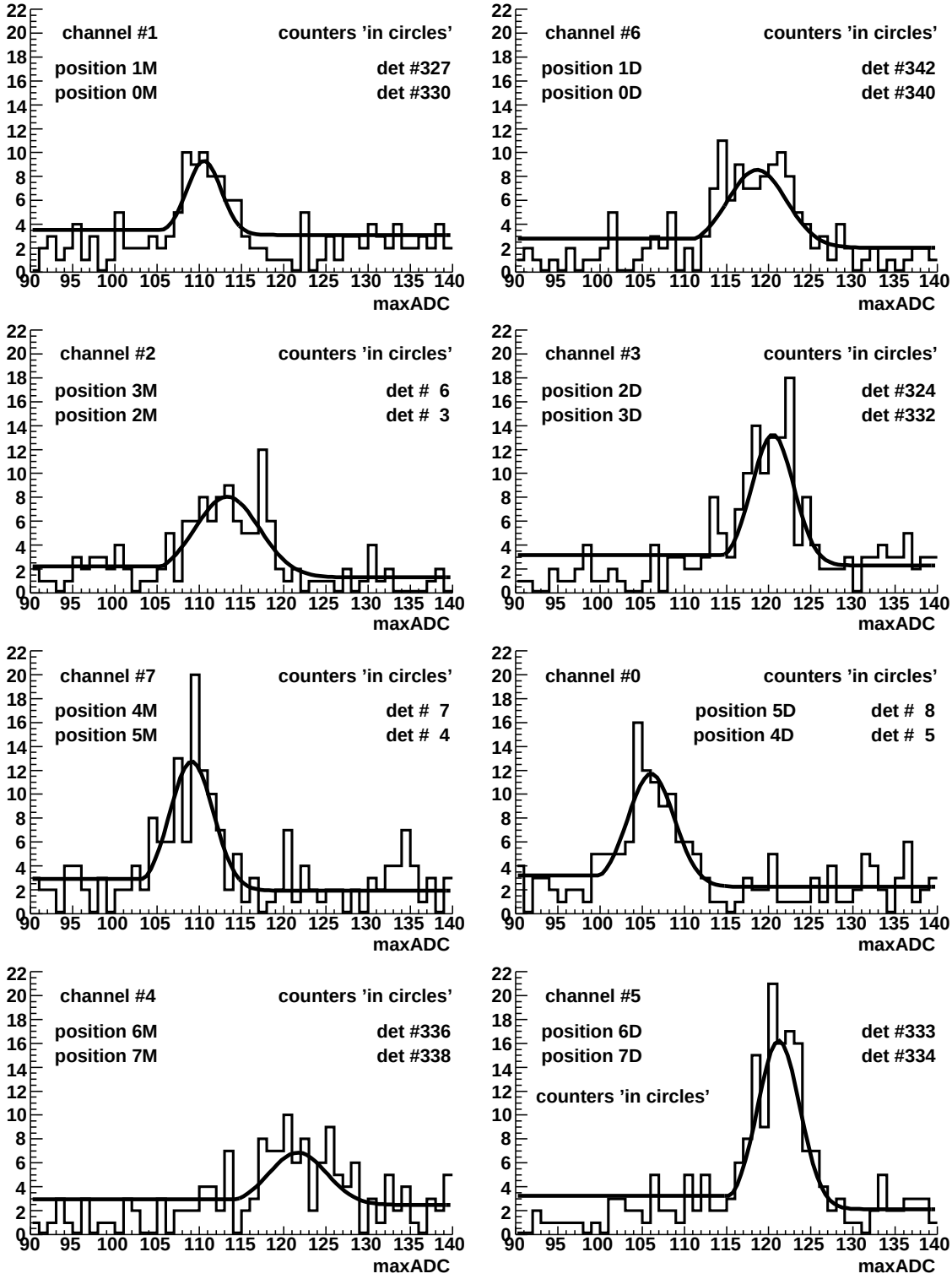

Figure 10: Neutron registrations in underground laboratory and detector setup 'in circles'. There are separate distributions for each ADC channel. Order of figures: left figures correspond to inner circle (labelled 'M'), and right figures correspond to outer circle (labelled 'D'). Pairs of detectors are connected to one channel.
Fit is sum of gaussian distribution for 764 keV peak, α background constant level (see Table 6), and 'wall effect'.

- constant value function corresponding to the α particle background as measured for ADC range 130–250 and shown in the Table 6 in the column "sum tunnel" and rows

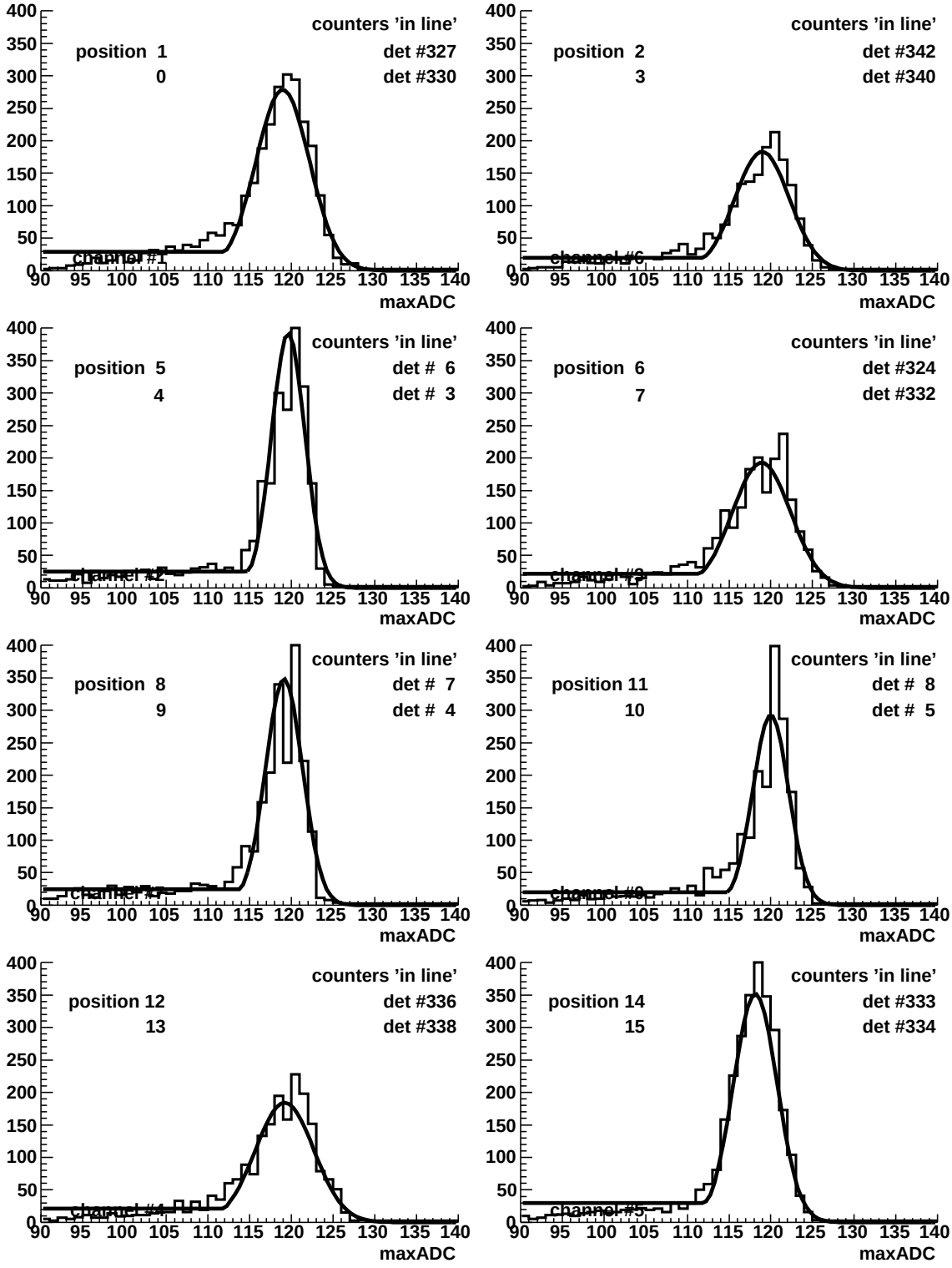

Figure 11: Neutron registrations in basements of surface laboratory building made before measurements in the tunnel and detector setup 'in line'. There are separate distributions for each ADC channel. Order of figures corresponds to detector setup 'in circles', in the Figure 10 and position of detectors in 'line' setup are indicated by numbers from 0 to 15. Pairs of detectors are connected to one channel.
Fit is sum of gaussian distribution for 764 keV peak, α background constant level (see Table 6), and 'wall effect'.

"rates per hour lifetime";

- gaussian function to describe 764 keV peak (as a sum from two ^{3}He counters);

- constant value function corresponding to 'wall effect' normalized in energy range 191 keV – 764 keV to the number of events within gaussian shape for the 764 keV peak (this part is used only below 764 keV peak, and only if its contribution is larger than the contribution from gaussian function).

The number of neutrons in 764 keV peak was obtained by sum of positive values of difference between histogram value and the expected α background for each histogram bin within ADC values for which the gaussian function fit to the 764 keV peak is larger than 0.5. The values are presented in the Table 7 for the ground level measurements made just before measurements in the tunnel (setup 'in line'), Table 8 for underground 'in line' measurements, and in Tables 9 and 10 for underground measurements 'in circles' setup for inner and outer circles respectively.

Table 7: Neutrons in 764 keV peak as the difference between sum of measured ADC histogram over the peak area and the constant α background. Data from results of measurements 'in line' at the surface level (first run from the Table 2).

FADC channel label	no in 'line'		^{3}He counter label		surface laboratory 'in line'			
					all events in 764 keV peak	α's in 764 keV peak	neutrons in 764 keV peak	neutron rate per hour
1	1	2	330	327	2515	2.07	2513.02	361.7
2	4	5	03	06	2100	0.59	2099.45	302.2
7	8	9	07	04	2071	0.94	2070.12	298.0
4	12	13	336	338	1864	1.80	1862.20	268.0
6	3	2	340	342	1676	1.36	1674.70	241.0
3	6	7	324	332	1931	1.67	1929.54	277.7
0	10	11	05	08	1766	1.09	1765.05	254.0
5	14	15	333	334	2660	1.22	2658.78	382.7
				sum	16583	10.74	16572.86	2385.3

Table 8: Neutrons in 764 keV peak as the difference between sum of measured ADC histogram over the peak area and the constant α background. Data from results of measurements 'in line' in the underground laboratory (second run from the Table 2).

FADC channel label	no in 'line'		^{3}He counter label		underground laboratory 'in line'			
					all events in 764 keV peak	α's in 764 keV peak	neutrons in 764 keV peak	neutron rate per hour
1	1	2	330	327	97	23.49	73.51	0.467
2	4	5	03	06	99	10.73	88.27	0.560
7	8	9	07	04	108	17.26	91.39	0.580
4	12	13	336	338	67	16.99	50.01	0.317
6	3	2	340	342	115	23.79	91.21	0.579
3	6	7	324	332	109	25.25	83.75	0.532
0	10	11	05	08	88	18.48	70.06	0.445
5	14	15	333	334	128	18.94	109.52	0.695
				sum	811	154.93	657.72	4.175

Table 9: Neutrons in 764 keV peak as the difference between sum of measured ADC histogram over the peak area and the constant α background. Data from results of measurements 'in circles' in the underground laboratory for the counters in inner circle (third run from the Table 2).

FADC channel label	no in 'circle'	^{3}He counter label	underground laboratory inner 'circle'			
			all events in 764 keV peak	α's in 764 keV peak	neutrons in 764 keV peak	neutron rate per hour
1	0M 1M	330 327	65	28.00	37.11	0.162
2	2M 3M	03 06	90	22.16	68.45	0.298
7	4M 5M	07 04	97	23.22	73.78	0.321
4	6M 7M	336 338	83	34.66	49.29	0.215
		sum	335	108.04	228.63	0.996

Table 10: Neutrons in 764 keV peak as the difference between sum of measured ADC histogram over the peak area and the constant α background. Data from results of measurements 'in circles' in the underground laboratory for the counters in outer circle (third run from the Table 2).

FADC channel label	no in 'circle'	^{3}He counter label	underground laboratory outer 'circle'			
			all events in 764 keV peak	α's in 764 keV peak	neutrons in 764 keV peak	neutron rate per hour
6	0D 1D	340 342	99	32.63	68.45	0.298
3	2D 3D	324 332	111	29.89	81.41	0.355
0	4D 5D	05 08	104	31.42	72.58	0.316
5	6D 7D	333 334	131	27.60	103.53	0.451
		sum	445	121.53	325.97	1.420

Still without determining the value of neutron flux, it is possible to estimate lower limits of neutron rate which can be measured with this equipment. In the Tables 8, 9 and 10 we have shown total number of events within the max ADC range of 764 keV neutron peak, extrapolated background due to internal α emission, evaluated number of neutrons in the peak and neutron rate per hour.
From the Table 8 we can see, that for one week measurements the 10 times smaller neutron flux is about the lower limit of this equipment. For measurements of MeV range neutron flux, using moderators, this estimation needs to be modified, and would be about twice as high as for thermal neutrons (in this case).

G Simulations of neutron measurements.

Simulations were made using GEANT4 toolkit [1]. There were two different targets for simulations:

- simulations of efficiency of neutron registrations in single ^{3}He neutron counter placed in an experimental setup and for neutrons emitted from AmBe neutron source, in

Table 11: Results of GEANT4 simulations of ^{3}He counters efficiencies in detector layouts 'in line' and 'in circles' with assumption of constant ^{3}He gas pressure (4 atm) and ^{3}He gas pressure adjusted following calibration measurements.
Neutrons with energy 0.024 eV were emitted from the sphere with radius 3 m. The idea of simulations is illustrated in the Fig. 8.
Number of registered neutrons includes all neutrons reacting with ^{3}He (equation 1), i.e. both in 764 keV peak and in 'wall effect'. Statistical error is less than 2%.

$10^7\times$ number of emitted neutrons:				setup 'in line'		setup 'in circles'		
				7.3839	6.8	9.849	8.673	
				simulated number of registered neutrons				
FADC channel label	^{3}He counter label	# 'line'	# 'circles'	with constant pressure	with adjusted pressure	with constant pressure	with adjusted pressure	adjusted pressure (atm)
1B	330	0	0M	3629	3254	2487	2236	3.64
1A	327	1	1M	3486	3197	2531	2395	3.91
2B	03	4	2M	3492	2844	2551	2136	3.22
2A	06	5	3M	3566	3087	2580	2091	3.36
7A	07	8	4M	3430	2798	2539	2028	2.85
7B	04	9	5M	3496	2987	2475	2092	3.22
4A	336	12	6M	3472	3158	2531	2192	3.58
4B	338	13	7M	3512	2778	2563	1947	2.95
6B	340	3	0D	3523	3119	3377	2944	3.64
6A	342	2	1D	3547	3084	3444	2842	3.58
3A	324	6	2D	3607	3082	3397	2881	3.71
3B	332	7	3D	3567	3332	3425	3024	3.64
0B	05	10	4D	3483	2659	3435	2479	2.90
0A	08	11	5D	3496	2717	3433	2595	2.80
5A	333	14	6D	3563	3211	3493	2974	3.77
5B	334	15	7D	3616	3483	3337	3169	4.42

order to compare results of simulation with measurements and validate the simulation code as a tool for interpretation of experiment;

- simulations of efficiency of thermal neutron registrations in a set of ^{3}He neutron counters in configurations 'in line' and 'in circles' in order to estimate neutron flux from neutron registrations.

The first target helps to understand some differences between detectors. We found and took into consideration

- different ^{3}He gas pressure responsible for neutron registrations in process described in equation 1 and also might have influence on other detector shielding in 'circles' layout;
- fractions of neutrons registered with amplitudes in the 764 keV peak and in the 'wall effect' range depend on counter geometry and ionisation range of proton and tritium in internal gas; fraction of neutrons in the 764 keV peak can be measured; in case of detectors used in LNGS ionisation range depends on pressure of krypton gas with nominated (original) pressure 0.5 atm; however in comparison with GEANT4 simulations we also used another counters without stopping gas, i.e. ionisation range as well as efficiency depend on ^{3}He gas pressure.

G.1 Simulations of efficiency of single ^{3}He neutron counter.

We built experimental setup to test separately ^{3}He neutron counters and compared observed counting rates with expected from GEANT4 simulations. In the center of 24 m^2

Table 12: Number of registered neutrons per 10^6 neutrons emitted with energy 0.024 eV from the sphere with radius 3 m as results of GEANT4 simulations of ^{3}He counters efficiencies in detector layouts 'in line' and 'in circles' with assumption of constant ^{3}He gas pressure (4 atm) and ^{3}He gas pressure adjusted following calibration measurements.
The idea of simulations is illustrated in the Fig. 8.
Number of registered neutrons includes all neutrons reacting with ^{3}He (equation 1), i.e. both in 764 keV peak and in 'wall effect'. Statistical error is less than 2%.

FADC channel label	^{3}He counter label	# 'line'	# 'circles'	simulated number of registered neutrons from 10^6 emitted neutrons				adjusted pressure (atm)
				setup 'in line'		setup 'in circles'		
				with constant pressure	with adjusted pressure	with constant pressure	with adjusted pressure	
1B	330	0	0M	49.15	47.85	25.25	25.78	3.64
1A	327	1	1M	47.21	47.01	25.70	27.61	3.91
2B	03	4	2M	47.29	41.82	25.90	24.63	3.22
2A	06	5	3M	48.29	45.40	26.20	24.11	3.36
7A	07	8	4M	46.45	41.15	25.78	23.38	2.85
7B	04	9	5M	47.35	43.93	25.13	24.12	3.22
4A	336	12	6M	47.02	46.44	25.70	25.27	3.58
4B	338	13	7M	47.56	40.85	26.02	22.45	2.95
6B	340	3	0D	47.71	45.87	34.29	33.94	3.64
6A	342	2	1D	48.04	45.35	34.97	32.77	3.58
3A	324	6	2D	48.85	45.32	34.49	33.22	3.71
3B	332	7	3D	48.31	49.00	34.78	34.87	3.64
0B	05	10	4D	47.17	39.10	34.88	28.58	2.90
0A	08	11	5D	47.35	39.96	34.86	29.92	2.80
5A	333	14	6D	48.25	47.22	35.47	34.29	3.77
5B	334	15	7D	48.97	51.22	33.88	36.54	4.42

room we made from graphite blocks a 'well'. Walls of the well were 20 cm thick and 70 cm high. Inside the well there was a water moderator (20 litres). We placed ^{3}He proportional counter inside the well. The counter was connected to different FADC: 16 MHz sampling rate, 8 bit ADC range and in every event 256 samples of wave form we put to computer memory. The voltage amplitude trigger level is adjustable and was set below the value corresponding to 191 keV lower limit of reaction 1 of neutron registration in ^{3}He. The data acquisition system is able to register more than 1000 events per second.

For each counter we performed two runs: one with AmBe neutron source inside the well and the second without the source. The AmBe neutron source emits about 200 neutrons per second. Energy spectrum of AmBe neutron source is known from the literature [2]. Subtraction of background neutron rate from the neutron rate with AmBe source gave us the registration rate and amplitude distribution of neutrons from AmBe source.

Measurements were done for counters used in LNGS measurements and with other larger ^{3}He counters made without stopping gas. For counters used in LNGS resulting counting rates, fraction of neutrons in the 764 keV peak and peak width are presented in Tables 5, 4 or 3.

Measurements and simulations made for detectors without stopping gas enable us to correlate two observed and simulated features related directly to the ^{3}He gas pressure: counting rate (efficiency of neutron registration) and fraction of neutrons in the 764 keV

Table 13: Expected number of registered neutrons per hour if the thermal neutron flux is equal to 10^{-6} neutrons per (cm^2 s). These are results of GEANT4 simulations of ^{3}He counters efficiencies in detector layouts 'in line' and 'in circles' with assumption of constant ^{3}He gas pressure (4 atm) and ^{3}He gas pressure adjusted following calibration measurements.
Neutrons with energy 0.024 eV were emitted from the sphere with radius 3 m. The idea of simulations is illustrated in the Fig. 8.
Number of registered neutrons includes all neutrons reacting with ^{3}He (equation 1), i.e. both in 764 keV peak and in 'wall effect'. Statistical error is less than 2%.

FADC channel label	^{3}He counter label	# 'line'	# 'circles'	simulated neutron rate per hour assuming neutron flux $10^{-6}\frac{n}{cm^2 s}$				adjusted pressure (atm)
				setup 'in line'		setup 'in circles'		
				with constant pressure	with adjusted pressure	with constant pressure	with adjusted pressure	
1B	330	0	0M	0.800	0.779	0.411	0.420	3.64
1A	327	1	1M	0.769	0.766	0.419	0.450	3.91
2B	03	4	2M	0.770	0.681	0.422	0.401	3.22
2A	06	5	3M	0.787	0.739	0.427	0.393	3.36
7A	07	8	4M	0.757	0.670	0.420	0.381	2.85
7B	04	9	5M	0.771	0.715	0.409	0.393	3.22
4A	336	12	6M	0.766	0.756	0.419	0.412	3.58
4B	338	13	7M	0.775	0.665	0.424	0.366	2.95
6B	340	3	0D	0.777	0.747	0.558	0.553	3.64
6A	342	2	1D	0.782	0.739	0.569	0.534	3.58
3A	324	6	2D	0.796	0.738	0.562	0.541	3.71
3B	332	7	3D	0.787	0.798	0.566	0.568	3.64
0B	05	10	4D	0.768	0.637	0.568	0.466	2.90
0A	08	11	5D	0.771	0.651	0.568	0.487	2.80
5A	333	14	6D	0.786	0.769	0.578	0.558	3.77
5B	334	15	7D	0.798	0.834	0.552	0.595	4.42

peak (as ionisation losses are due to ^{3}He in that case).
The absolute values of counting rate and fraction of neutrons in the 764 keV peak in measurements and simulations are in agreement with 99% accuracy. Most of neutrons emitted from AmBe source are in 1–10 MeV range. Transport, thermalisation and registrations are very well simulated by GEANT4.

For ^{3}He counters used in LNGS we have measured different counting rates for neutrons from AmBe source (see Tables 5, 4 or 3). These counters are relatively old and it is rather likely that ^{3}He gas pressure might be different from nominal 4 atm. We estimated ^{3}He gas pressure for each counter separately to reach agreement between simulation results and measured counting rate for neutrons emitted from AmBe source. Gas pressures are shown in the Tables 11, 12 or 13.
Influence of adjusted ^{3}He gas pressure on final result of thermal neutron flux measurements can be seen in the Figure 12 by comparison of points connected by solid lines in upper figures.

G.2 Simulations of expected counting rate for LNGS measurements.

Simulations of expected thermal neutron counting rate (efficiency) were performed using GEANT4 toolkit and with a scheme illustrated in the Figure 8. Neutrons were emitted from the sphere uniformly and isotropically. Sphere radius was 3 meters, which ensure

uniform and isotropic neutron flux in the volume occupied by detectors (in the center of the sphere) with accuracy of 1%.
The neutron energy was constant and equal to 0.024 eV – the average energy for temperature 5°C. We do not know, where neutrons were thermalized in experimental conditions: inside the rock (we do not know temperature there), or inside underground laboratory in tons of poliethylene placed around. For 20°C the average energy is 0.025 eV and the reaction cross section (equation 4) is about 2% smaller than for 0.024 eV (5°C) – our measurement accuracy is poorer.

We performed simulations for two detector layouts: 'in line' and 'in circles'. And for each case we simulated two conditions: the same ^{3}He gas pressure equal to 4 atm, and with individually set in each counter according to values presented in the Tables 11, 12 or 13. Results of simulations are presented in the Table 11. Then in Table 12 we present efficiency: number of registered neutrons per 10^6 emitted from the sphere for each case. Finally, in the Table 13 results are normalised: neutron emission rate corresponds to the neutron flux of 10^{-6} neutrons/(cm^2 s) and results are presented in expected neutron rate per hour for each ^{3}He counter. To compare simulations with measurements (Figure 12) simulated registration rate in each detector was multiplied by fraction of neutrons in the 764 keV peak (either the same for all counters and equal to 0.63 or individually measured and presented in the Table 3) to obtain expected rates of neutrons in peak, as measured. Then rates were summed in pairs connected to the same channel. Expected rates are presented in the Figure 12 as smaller points connected by solid lines.

Fraction of neutrons observed in the 764 keV peak was not included in GEANT4 simulations for detectors used in LNGS. All neutrons reacting with ^{3}He were counted in simulations. The factor related to fraction of neutrons in the 764 keV peak was applied before comparison with measurements. The role of this factor is relatively large, what can be seen while examining simulation points (connected by solid lines) in left Figures 12, where in lower–left figure measured factors related to individually measured fractions of neutrons in peak had been applied.

H Thermal neutron flux estimation – role of simulation.

Simulations with GEANT4 toolkit we made for 'in line' and 'in circles' layouts. We made simulations for the same ^{3}He gas pressure and for different pressure in each counter. The pressures were adjusted to measured difference in counting rates during calibration measurements (see Tables 3, 4 or 5). For comparison with measurements in the tunnel simulations were performed for neutrons with energy 0.024 eV escaping isotropically from the sphere (see Figure 8).

In simulation neutron registration takes place when neutron is lost in reaction 1 inside the ^{3}He counter. Therefore comparison with measurements requires another factor related to the "wall effect": ratio of neutrons in the 764 keV peak to all registered neutrons. This ratio was measured for each detector and values are in the Tables 3, 4 or 5.

The neutron flux was obtained as weighted average of $f_{\delta\ i} \cdot F_A$ (equation 2) with different assumption about expected neutron counts, and weights are statistical significance of measured number of neutrons in the peak. We use different assumption about ^{3}He gas pressure and fraction of neutrons in the 764 keV peak to see influence of this assumption on the resulting neutron flux.

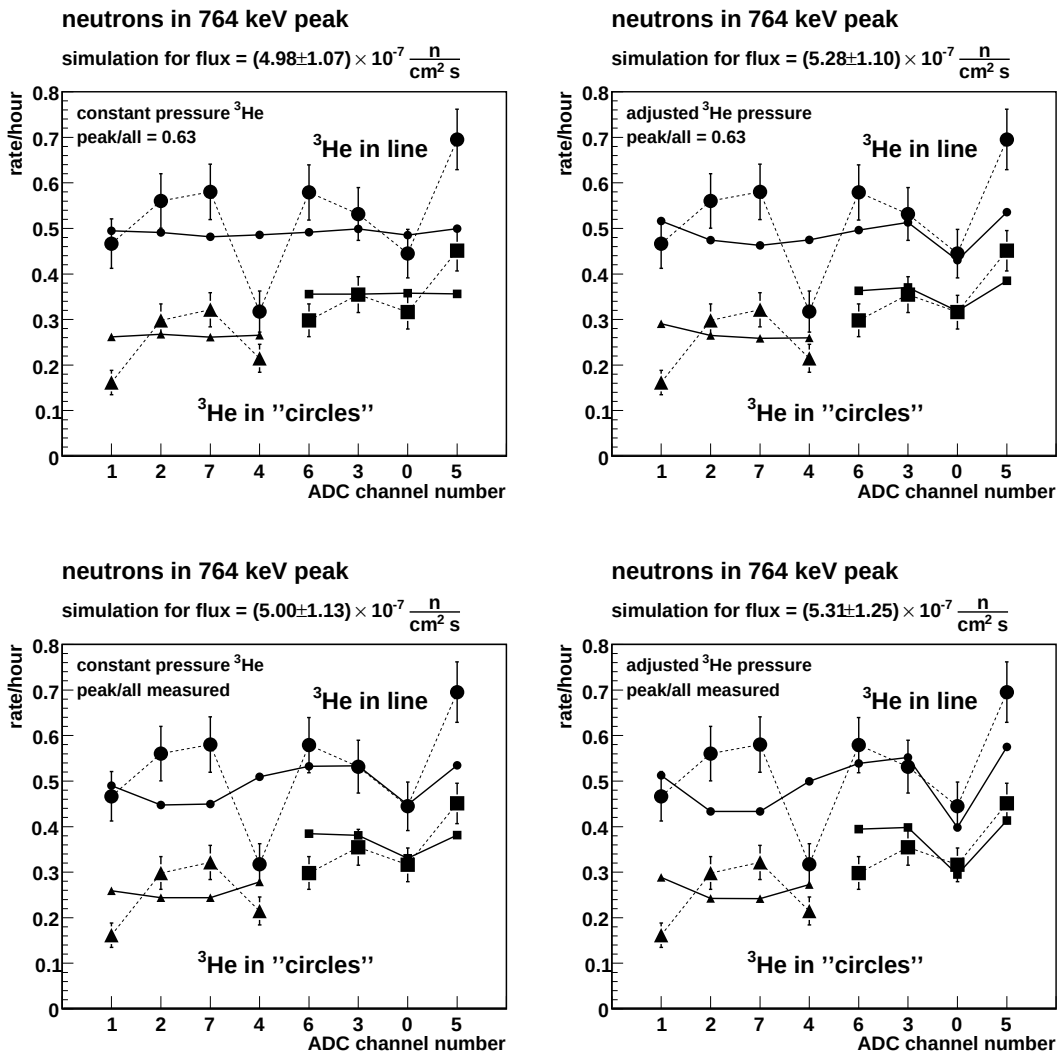

Figure 12: Comparison of observed number of neutrons with expected values from simulations. Simulations were made for four conditions to examine influence of these conditions on the estimated neutron flux. The conditions are constant or variable ^{3}He gas pressure inside the counter and constant or variable ratio of number of neutrons in 764 keV peak to all neutrons captured in the detector. First 4 channels from the left correspond to inner circle in 'circle' layout. The right bottom figure is our final result.
The best value of neutron flux was obtained for each figure as the weighted mean of $f_{\delta\ i} \cdot F_A$ (equation 2) from both runs in the tunnel presented in the figure (i.e. 'in line' and 'in circle').

The best result is the one where simulations were corrected for the individually evaluated ^{3}He gas pressure in each detector and with the individually measured fraction of neutrons in the peak.

In the Figure 12 we present rates of neutron registration and rates of simulated neutrons normalized to the best neutron flux. The points are for the same counter/channel for all measurements and expected values. First 4 channels from the left were connected to the inner circle counters for 'in circles' layout. Experimental points are the same in all four figures. The top left figure has no pressure corrections and constant fraction of neutrons in the 764 keV peak. Comparison of top figures shows the influence of different gas pressure on expected results in simulations (see Table 11, 12 or 13). Comparison of left figures shows the influence of different fraction of neutrons in 764 keV peak. This fractions were measured, and results are in Tables 5, 4 or 3. Both corrections were included in simulation

results presented in the right bottom figure, and this is our best result.

The estimated best neutron fluxes in each case are not very different, and are within errors.